



**13<sup>TH</sup> CANADIAN MASONRY SYMPOSIUM**  
**HALIFAX, CANADA**  
**JUNE 4<sup>TH</sup> – JUNE 7<sup>TH</sup> 2017**



---

**PRELIMINARY TESTS ON THE LATERAL LOAD-BEARING CAPACITY OF SLENDER  
MASONRY WALLS**

**Vermeltoort A.T.<sup>1</sup> and Martens D.R.W.<sup>2</sup>**

**ABSTRACT**

The lateral load bearing capacity of masonry walls depends mainly on its slenderness and the applied axial load. Often the lateral load is not critical but when seismic activity, caused by the winning of natural gas, becomes perceptible, this is no longer the case. Seismic actions cause vibrations in walls which induce lateral forces, varying in time. To study the behaviour of walls under lateral loads, a test set-up was developed. This paper discusses practical aspects of this set-up and the results of preliminary tests on 100 mm thick unreinforced masonry walls. In these tests, the axial load, representing loading by floor loads, was kept as constant as possible during each test. At mid-height of the wall, the out-of-plane deformation, was controlled. At that position, the test wall was cyclically pushed and pulled over a distance of up to 50 mm. In this three point bending test set-up the behaviour was governed by a three hinged rigid body mechanism, as expected. The tests showed the effects of different axial load levels. The lateral resistance of walls increases when axial loads are higher. In the preliminary tests, resemblance is found between experimental and analytical results. After some improvements, the full experimental program, which involves both unreinforced and strengthened masonry walls, under dynamic cyclic loading, will be performed.

**KEYWORDS:** *cyclic load, axial load, out-of-plane behavior, test set up, boundary condition*

**INTRODUCTION**

Earthquakes are becoming a common problem in Groningen, an area which is located in the North East of the Netherlands. These earthquakes are so called “induced earthquakes” which means that they are not caused by movement of tectonic plates (tectonic earthquakes) but by human activities such as drilling for oil or, like in Groningen, natural gas. These induced earthquakes cause subsidence of the ground and consequently deterioration of buildings in the Groningen region.

This gave reason to investigate the effect of cyclic loading due to moderate earthquakes and to what extent cyclic lateral loading would cause deterioration of masonry piers and walls. One main

---

<sup>1</sup> Eindhoven University of Technology, The Netherlands, a.t.vermeltoort@tue.nl

<sup>2</sup> Eindhoven University of Technology, The Netherlands, d.r.w.martens@tue.nl

question is in which cases masonry walls must be strengthened and how strengthening techniques, developed by e.g. Türkmen et al [1] will perform.

### ***Problem, type of construction***

The building tradition in the Netherlands evolved over the past century from massive walls, with a thickness equal to the length of a brick unit (approximately 21 cm), to a double leaf cavity wall with leaf thicknesses of approximately 100 mm and a cavity width of up to 150 mm, partly filled with insulation material (100 mm). This results in a total outer wall thickness of 350 mm.

The relatively thin leaves are designed for relatively moderate wind loads but not for seismic loading. Thickness, mass, axial loading and boundary conditions play a role in the capacity against seismic loading.

Due to lateral loading, e.g. by an earthquake, a wall starts to deflect (or vibrate) perpendicular to its surface with bending moments as a result. The capacity of masonry against bending depends mainly on the axial loading while tensile (bond) strength is usually small. The axial loading provides some pre-compression which compensates the tensile stresses caused by bending.

### ***Contents of paper / research goal***

The paper describes a test set-up, developed to investigate the effects of “cyclic lateral loading”. Small walls were tested with different pre-compressive axial loads to gain insight in the decreasing lateral stiffness. It is found that masonry piers with a higher pre-compression are able to resist a higher lateral load. In all cases, a system of two ridged bodies developed.

## **THEORY**

A wall can be seen as a structural element, in this case loaded both in axial direction and in lateral out-of-plane direction. The lateral load could be a result of movements during an earthquake or wind pressure.

Hendry et al. [2] describes the relationship between lateral strength and pre compression of story high walls of various thickness and materials. Figure 1 shows an increase in lateral resistance for all walls up to a pre-compression of about 2 MPa. The results for walls of 105 mm thickness are most in comparison with the topic of research in this paper.

Other tests on laterally loaded walls were conducted by Hendry, as described in Hendry et al. [2], in which the behavior due to an explosion was simulated. Comparing the results of this short dynamic loading with a slowly increasing load no significant difference was observed.

The studies described in Hendry et al. [2], Drysdale et al. [3] and MacDowell et al. [4] show that the effect of lateral loading on a wall can be studied using a mechanical scheme as shown in Figure 2. In this study, the usually used uniform load distribution is replaced by a point load. In the explorative experiments this way of loading was applied. In a test this is a line load.

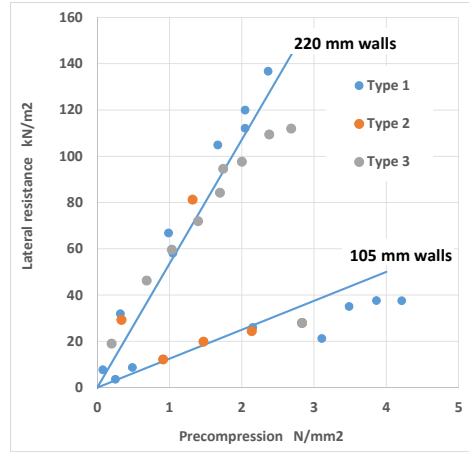


**Figure 1: Lateral resistance of brick walls vs pre compression (redraw from Hendry [2])**

Walls are usually clamped between floors. In the Groningen region, floors are often relatively light and carry relative small loads. Consequently, axial stresses in the order of magnitude of 1 MPa or less are common.

Increasing the lateral, out-of-plane force, creates cracks at positions where bending moments are largest, i.e. at the supports and at mid span. Eventually, a three hinged failure mechanism with two ridged bodies, as shown in Figure 2, develops, assuming horizontal reactions can be resisted. When the tensile bond strength of the mortar is neglected and no local crushing takes place at the hinges, the lateral load is given by equation 1.

$$H = 4 * N * \frac{t-2\alpha x-\delta}{h} \quad (1)$$

Where:

- t = wall thickness of wall
- h = height of wall
- x = width of compressed area
- H = applied lateral load
- N = applied axial load
- $\delta$  = mid span deflection
- $\alpha$  = factor depending on the shape of compressive stress strain curve

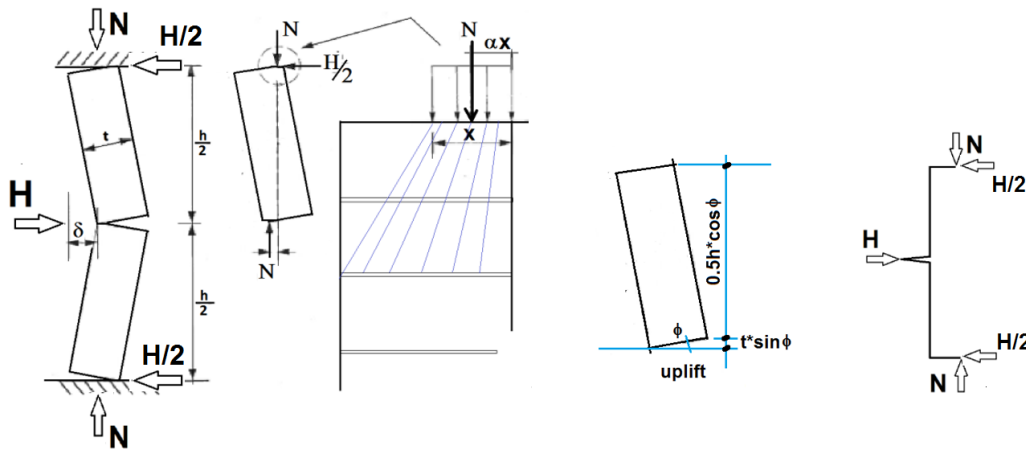


**Figure 2: Mechanical scheme of lateral point load on a wall**

Equation 1 shows the two main parameters in the lateral load bearing capacity, i.e. deflection ( $\delta$ ) and axial load (N). When small axial loads are present, the system can only resist relatively small lateral loads and the support frame (i.e. the whole building) can usually resist these forces easily. The axial load also has its effect of the size of the compressed area (x). With increasing deflection the size of the compressed area decreases and stresses increase, until the compressive strength of the masonry is reached. The ultimate deflection equals t, i.e. when the size of the compressed zone is assumed to be negligible small.

For a certain axial load, the depth of the compressed zone depends on the deflection. With a higher mid span deflection the depth of the compressive contact area decreases. The system has three critical spots, at mid-height, at the bottom and at the top where the effects of the decreasing compressed area are most visible. In the ultimate situation, the contact between two bodies is minimal.

Figure 3 shows, in a scheme, the lateral load plotted against the deflection  $\delta$  as measured in an experiment and against the load deflection relationship for rigid body behavior ( $\alpha x = 0$ ).

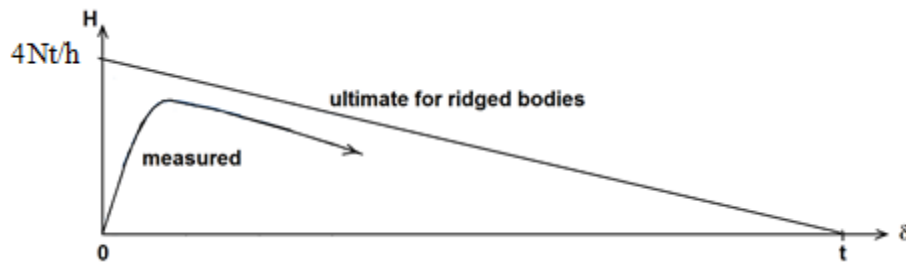


**Figure 3: Measured H vs delta and theoretical ultimate, schematic**

### ***Uplift***

When the wall is represented by two infinitely stiff prismatic bodies on top of each other the uplift (u) equals:

$$u = 2 * (\sqrt{((0.5h)^2 - \delta^2)} + \delta * t/0.5h) \quad (2)$$

Using equation (2) the estimated uplift for a displacement  $\delta = 25$  mm and  $h = 1250$  mm equals 7.0 mm. However, the bodies will get shorter due to the axial load, mainly in the cracked areas. For the relatively small axial loads used in this study, in the ultimate situation, the compressed area will be small. For an axial load of 70 kN, a specimen's width of 425 mm and a compressive strength of 10 MPa the width of the compressed area is 16.5mm. The relatively high stresses in the contact area will spread out. Assume, that at a distance equal to the thickness of the wall the stress distribution is almost uniform, Figure 2. The extra shortening of this piece of the specimen is estimated as 0.1 mm per crack. With four of these situations, this results in a net uplift of approximately 6.5 mm.

Also bending, however negligible small, will occur in the bodies. The shortening due to centric loading does not contribute to the uplift because the situation with axial load but without lateral load is considered as the starting situation.

## TEST SET-UP

### *Model of specimen in test set-up*

Above we have seen that the axial load is an important parameter. Therefore masonry test walls are loaded in axial direction. This axial load represents the top load on a masonry wall normally caused by floors and walls above. Three axial load levels, related to loads which can be expected in the Groningen region are used in the experiments. The lateral load is applied as a line load at mid-height. This load represents the horizontal actions normally caused by wind or earthquakes.

### *Material properties*

Six test walls have been built for the experiments from calcium silicate units with dimensions of 210×100×52 mm ( $l \times w \times h$ ) and thin bed mortar joints with a thickness of approximately 3 mm. The test walls were 22 courses high, 1210 mm. The width of the wall was equal to 2 units and one joint, 425 mm, Figure 4. The top and bottom courses were applied after the wall was placed in the test set-up. These gypsum layers were approximately 5 mm thick and created a tight contact between the bricks and the beam on top. Bond between steel load platen and gypsum is considered negligible.

### *Brick and mortar Properties*

In order to determine the properties of the units, twelve calcium silicate sample units were tested in compression. The mean compressive strength was 12.21 MPa, with a C.o.V. of 5.2 %.

Three mortar prisms were made from the thin bed mortar used for the Calcium Silicate walls. These prisms were tested in three point bending and compression according to EN – 1015-11. The average modulus of rupture for the three specimens was 3.79 MPa and the characteristic compressive strength of the remaining six prism parts was 15.65 MPa with a C.o.V. of 3.2%.

### *Test series*

The six identical test walls were divided in three test series of two specimens. In each series a different axial load was applied, with pre-stress target values of 0.12 MPa, 0.625MPa and 1.75 MPa. The calculated shortening is based on an E-value of 6000 MPa. The actual E-value of the test walls was established experimentally as discussed later in this paper.

**Table 1: Test program with intended axial loads and boundary conditions**

Type	Axial Load kN	Pre-stress* MPa	Shortening mm	based on E = 6000 MPa and length l = 1250 mm.
1	5.1	0.12	0.021	
2	26.4	0.62	0.121	
3	74.3	1.75	0.314	

\* based on a gross section area of 425 x 100 mm<sup>2</sup>

### ***Loading beam prevents rotation***

To test the walls, a rigid frame was built from the available steel beams with connection holes at regular distances. A separate frame was used to mount some of the measuring devices preventing that the test frame affected the results.

The front view of the test frame (Figure 4) shows a rectangle of two columns and two beams made from HE300B profiles. The side view shows, as main feature, a HE300B Beam, with a hinged connection at one end and resting on the test wall at the other end via steel plates and a beam. In this way, rotation of the specimen's top end was prevented. This connection simulated the floor-wall connection. At the bottom, the test wall rested on a steel HE300B beam with stiffeners between the flanges also to prevent rotation.

In the test frame, two jacks were mounted. One simple hydraulic jack, #1, which was used to apply the vertical load and one more sophisticated jack, #2, used to apply the lateral load in pull and push cycles. This jack, #2, acted as a pendulum (bar hinged at both ends). Jack #2 had its own hydraulic, automated control system which allowed to apply an easy cyclic loading program. While running the test it was possible to make changes or to abort the program if required.

The load from this horizontal jack #2 was transferred to the specimen by means of a steel bracing as shown in Figure 5. This bracing allowed to pull and push with negligible play and was made from two steel 40 x 40 mm<sup>2</sup> bars connected with M12 bolts at both ends.

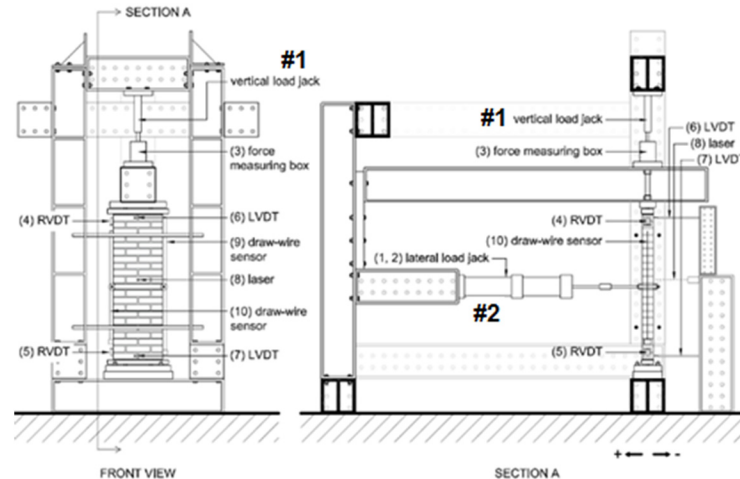


**Figure 4: Scheme of the test set-up with measuring devices.**

Jack #1 was hydraulically connected with a separate jack, #3, placed in a 250 kN machine. This jack #3 was loaded by this machine and the control equipment of this 250 kN machine was used to control the axial load. After applying the axial load the lateral loading program started. In subsequent cycles the specimen was given a lateral displacement in pull and push direction with a constant speed. Cycles had a saw tooth shape with the same duration, the maximum amplitude of

the displacement increased per cycle, in steps of 5 mm, till a maximum of 30 mm, i.e. seven cycles were applied. The maximum displacement measured on the specimen was 25 mm.

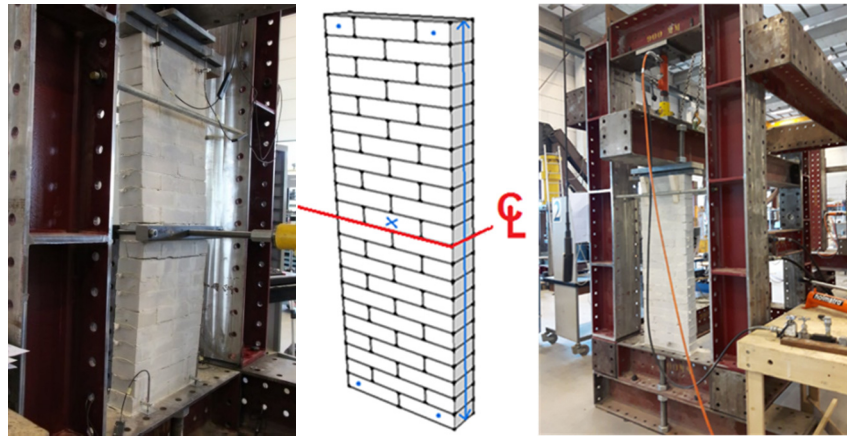
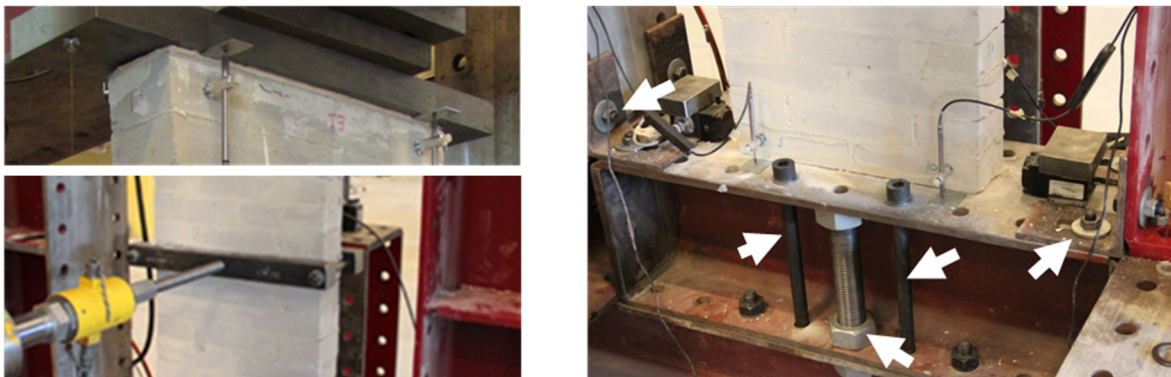


**Figure 5: Test wall, 425 mm long, 22 courses high, 100 mm thick in test set-up**

### ***Instrumentation***

The applied loads were measured by load cells. Deformations and displacements were measured by two DWS and eight LVDTs. Draw wire sensors (DWS) are instruments that can measure changes in length over the full height of the specimen. One at both the left and right hand side of the wall were used, as shown in Figure 5. The lateral displacement at mid height of the test wall was measured by a Laser instrument. Therefore an aluminium sheet of 50 x 50 mm<sup>2</sup> was glued to the brick just above the bracing.



**Bolts and steel corners to stiffen bottom beam.**

**Figure 6 Gypsum layer at the top of a test wall, steel connector to load in lateral (horizontal) direction and measuring devices and beam stiffeners at the foot of the wall**

The deformation of top and bottom joints between wall and load platen was measured using eight LVDT's, one at each corner of the test wall. Changes in length from the upper or lower row of bricks to the steel loading platens were measured. From the results the rotation of the wall segments was computed. The LVDT's are indicated with the blue dots in Figure 4.

## RESULTS

### *Modulus of Elasticity*

Before applying lateral load, the walls type 3 (see Table 1) were axially loaded in compression to an averaged stress of 1.75 MPa and deformations measured. This allowed to establish the modulus of elasticity. For one wall the E-value was  $E = 7700$  MPa for the other wall  $E = 6600$  MPa.

### *Variation of axial load*

The axial load was measured by a load cell directly between the load beam and the hydraulic jack. As an example, the measured normal force versus time is plotted in Figure 7. The fluctuation followed the applied displacement (horizontal load). The N+ and N- values for all walls are given in Table 2.

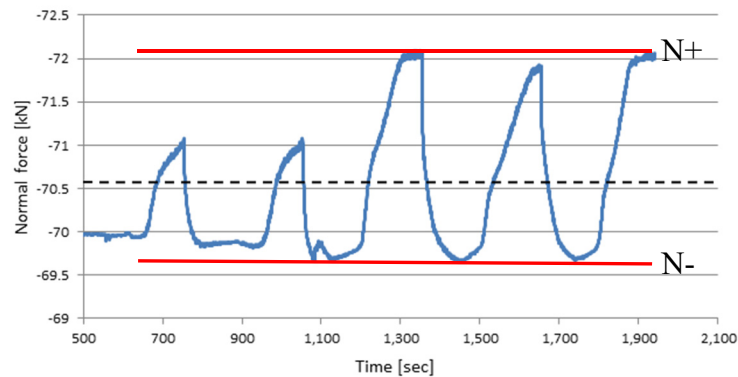


**Figure 7: Fluctuation of axial load in time due to uplift by horizontal movement**

### *Lateral load versus axial load*

Figure 8a shows the relationship between horizontal load and vertical axial load. For this graph the values from the final load cycles of each test were used.

The test walls all behaved in a similar manner. Three cracks were observed, located at the top and bottom support and at mid-height, close to the load application point, indicating that in this phase of the test the specimen can be considered as split in two ridged bodies. Using equation (1) and the accessory assumptions with rigid body behavior as mentioned earlier, the ratio  $H/N$  equals  $4 \cdot (t - \delta) / h$ . Substituting  $t = 100$  mm,  $\delta = 25$  mm, and  $h = 1250$  mm an  $H/N$  ratio of 0.24 is obtained. However, the test wall in the set-up had some minor deviations from the ideal situation which when taken into account together with the own weight, results in an  $H/N$  ratio of 0.253.

In each test, the absolute value of the ratio between horizontal load ( $H$ ) and axial load ( $N$ ) in both push and pull direction is equal i.e. symmetric behavior for push and pull. For small axial loads the  $H/N$  ratio is almost equal to the rigid body  $H/N$  ratio of 0.253. It is expected that some test set-up effects, like the connection of the loading beam and the horizontal jack have caused an additional, not measured, axial load. Also, the own weight of the wall is neglected in Equation (1). The found  $H/N$  ratios indicate that the compressed areas must have been relatively small. For larger axial loads

the H/N-ratios are larger, i.e. the compressed areas must have been larger too. The H/N ratio of walls #1 and #2 which were tested first, are out of line while in those two tests the bottom beam allowed more rotation.

### ***Horizontal displacements and uplift***

The horizontal displacements measured with the laser system were more direct than those from the LVDT on jack #2, used for control. In the direct control measurements not only the movement of the head of the jack was involved but also deformations in the jack system and connections. However, the laser system was mounted on a separate frame so some movement of the frame was included.

Figure 8b shows the measured uplift plotted against the applied axial force. A decreasing trend is visible because a larger axial load will induce more deformation in the areas where rotation occurs, i.e. in the contact joints and the crack at mid-height. Consequently, the uplift will be smaller. Only the magnitude of the horizontal deformation and not the direction affects the uplift. The measured uplift for an axial load of 70 kN is approximately 6.5 mm which is of the same order of magnitude as the earlier prediction using equation (2). The supports were more flexible for the first two tests with an axial load of approximately 20 kN and stiffened afterwards for the remaining four tests. That explains the smaller uplift for those two tests than expected according to the trend line in Figure 8b.

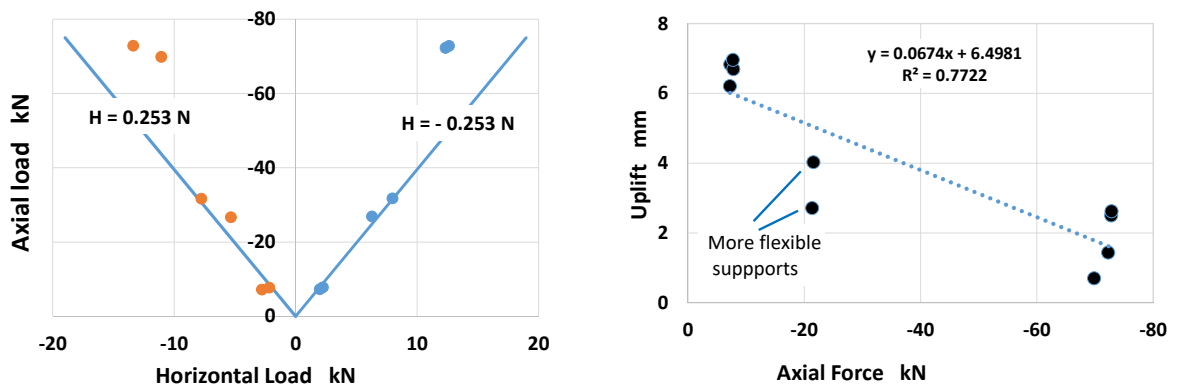


**Figure 8: a) Vertical load versus horizontal load, results from final cycles  
b) Measured uplift versus horizontal load**

### ***Stiffness of test walls***

To obtain an impression of the stiffness of the test walls, load-lateral deflection graphs were plotted using the measured results from the first load cycle. In most cases a kink in the first part of the graph was observed, indicating the cracking of the wall. The initial stiffness ( $k_i$ ) was estimated by using the slope of the linear first part in the graph (straight line in Figure 9). A second indication of stiffness was found in the slope of the line connecting the two end points of the loop ( $k_l$ ) of the first cycle. A third stiffness value,  $k_f$ , was obtained from the final loading cycle. In Table 2 the values for  $k_i$ ,  $k_l$  and  $k_f$  are presented. Wall 5 and 6 had the lowest axial load ( $N \sim 5$  kN) which explains

the lower stiffness compared to walls 3 and 4 ( $N \sim 70$  kN), and wall 1 ( $N \sim 25$  kN). The relatively low  $k_i$ -value of wall 2 is caused by practical issues during testing. However, the loop stiffness  $k_l$  of wall 2 is more in line with the value of the other tests 5 and 6.

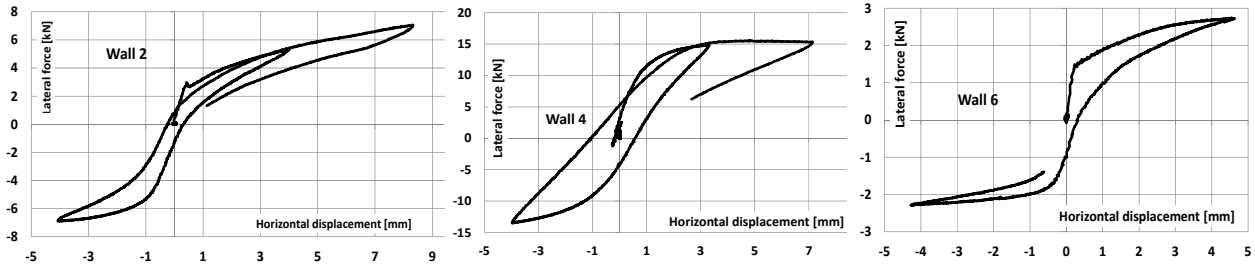


**Figure 9: Examples of load-lateral displacement graphs, first cycles.**

**Table 2: Axial and Horizontal Loads, stiffnesses and rotations at contact joint**

No.	N+	N-	H+	H-	$k_i$	$k_l$	$k_f$	Rot+	Rot-
	kN	kN	kN	kN	kN/mm	kN/mm	kN/mm		
1	8.1	6.8	-7.77	7.97	13.40	2.24	0.262	0.0538	-0.0461
2	7.4	6.4	-5.33	6.28	4.44	1.39	0.194	0.0547	-0.0486
3	72.1	69.7	-13.39	12.63	13.33	5.18	0.434	0.0551	-0.0526
4	72.7	69.8	-11.07	12.34	11.11	3.89	0.424	0.0563	-0.0509
5	21.7	19.5	-2.78	1.99	2.92	0.95	0.080	0.0548	-0.0555
6	26.8	23.3	-2.17	2.24	4.29	1.01	0.075	0.0543	-0.0534
								0.0548	-0.0512

\*) Loads in final cycle with lateral displacement of 25 mm

### Rotation

The maximum lateral displacement at mid-height was 25 mm (jack displacement 30 mm). With a wall height of 1250 mm this results in a rotation of  $25/625 = 0.04$ . The joint deformation, measured with LVDTs at top and bottom joint allowed to establish the rotation in the contact joint area. The measured rotations in the contact joint are given in Table 2. The variation is relatively small. The mean value is larger than the overall rotation of 0.04 of the two wall parts. This indicates that most of the deformation occurs in the contact joints/cracks and confirms the mentioned relatively small contact areas between the ridged bodies when lateral displacements are larger.

### DISCUSSION

This paper describes the development and characteristics of a test set-up for walls loaded both in axial and in lateral direction. To explore the possibilities of the test set-up, six 100 mm thick walls of 430 mm wide and 1250 mm high were loaded in cycles with increasing displacement per cycle. The axial load was intended to be constant during testing while the lateral load varied. Via displacement control the lateral displacement at mid height of the wall varied from -25 mm (pull) tot 25 mm (push) and consequently the lateral load varied depending on the applied axial load. The lateral loading was applied relatively slow compared to the dynamic nature of seismic loading but allowed a check of all features of the set-up and to study of behavior of the test walls.

During the subsequent testing of the six walls, some minor changes and additions on the test set-up were made, based on the gained experiences. In Test 1 the draw wire sensor (DWS) was added to measure the uplift. Also provisions were taken to allow the horizontal jack to act more like a pendulum (rotating end instead of fixed end connection). In Test 2 the way the axial load was introduced was changed. In this and subsequent tests, a seven mm thick gypsum joint was used between the wall end and the loading platen, both top and bottom, to allow for a smooth load introduction. In Test #3 the rotation of the flanges of the bottom beam was prevented by adding steel connector studs. Tests #4, #5 and #6 were done in a similar manner as test #3. Fluctuations of the axial load were observed during testing. This may be caused by friction in the jack.

## **CONCLUSIONS AND RECOMMENDATIONS**

A test set-up was developed and six specimens were tested to explore its performance. The system i.e. the combination of set-up and test wall, was sensitive especially when relatively small axial loads were applied. Another way to control of the axial force, must be considered.

Theoretical models confirmed the trends found in the experiments. A larger axial load results in a larger lateral load required for the same lateral deformation while the uplift is smaller. It can be concluded that a system of two (rigid) bodies can be used to predict the behavior.

Only six specimens were tested in the laboratory. It would be interesting to repeat the test with higher pre-compression and larger lateral displacements to allow confirmation of the theoretical relationships, and further, to improve the control of the axial load in order to minimize fluctuations during testing and to allow observation of specimens' behavior under relatively low axial loads.

## **REFERENCES**

- [1] Türkmen Ö.S., Vermeltoort A.T. and Martens D.R.W. 2016 Seismic retrofit system for single leaf masonry buildings in Groningen. Proc. 16<sup>th</sup> IBMaC, Padova, Italy.
- [2] Hendry A.W. 1990 Structural Masonry, Macmillan Education LTD, ISBN 0-333-49748-1.
- [3] Drysdale R.G. and Hamid A.A. 2008 Masonry structures Behavior and Design, 3th Edition, The masonry society Boulder Colorado ISBN 1-929081-33-2
- [4] MacDowell E.L. McKee K.E. and Sevin E. 1956 Arching action of masonry walls Proc. ASCE, J. Struct. Div. Vol. 82 (ST2) 1956 Paper 915.